Supplementary information for 'The interplay between growth rate and nutrient quality defines gene expression capacity'

by

Juhyun Kim, Alexander P.S. Darlington, Declan G. Bates
and Jose I. Jimenez

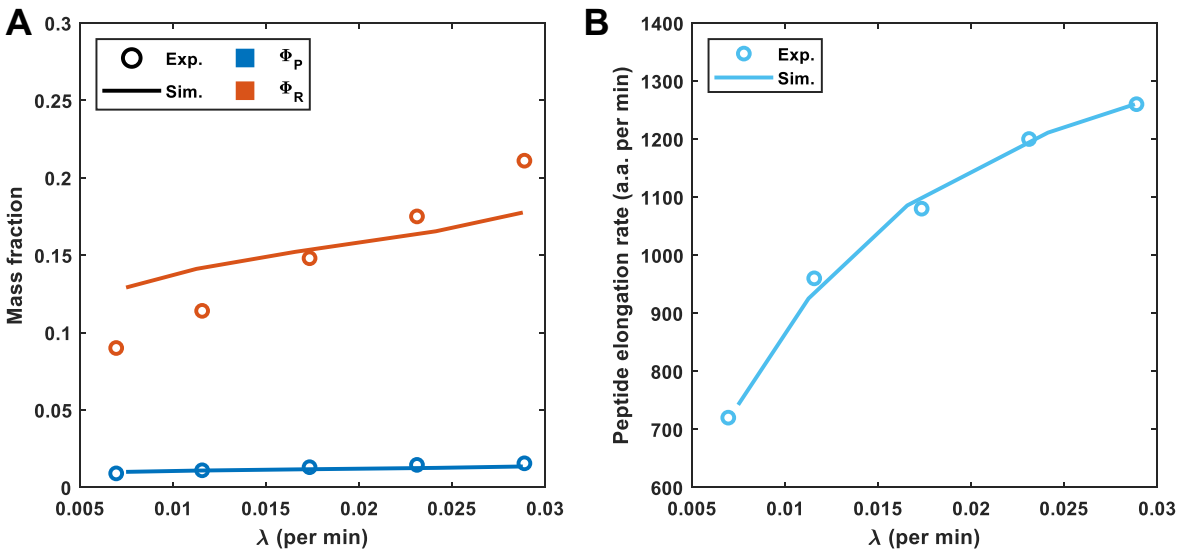

Figure S1. Quality of data fitting. (A) The model was fit as described in the main text. The simulated mass fraction of the RNA polymerase and ribosomes are shown with the experimental data from Bremer and Dennis (1996). **(B)** The peptide elongation values reported in the same publication were not used in the data fitting but simulations show good agreement.

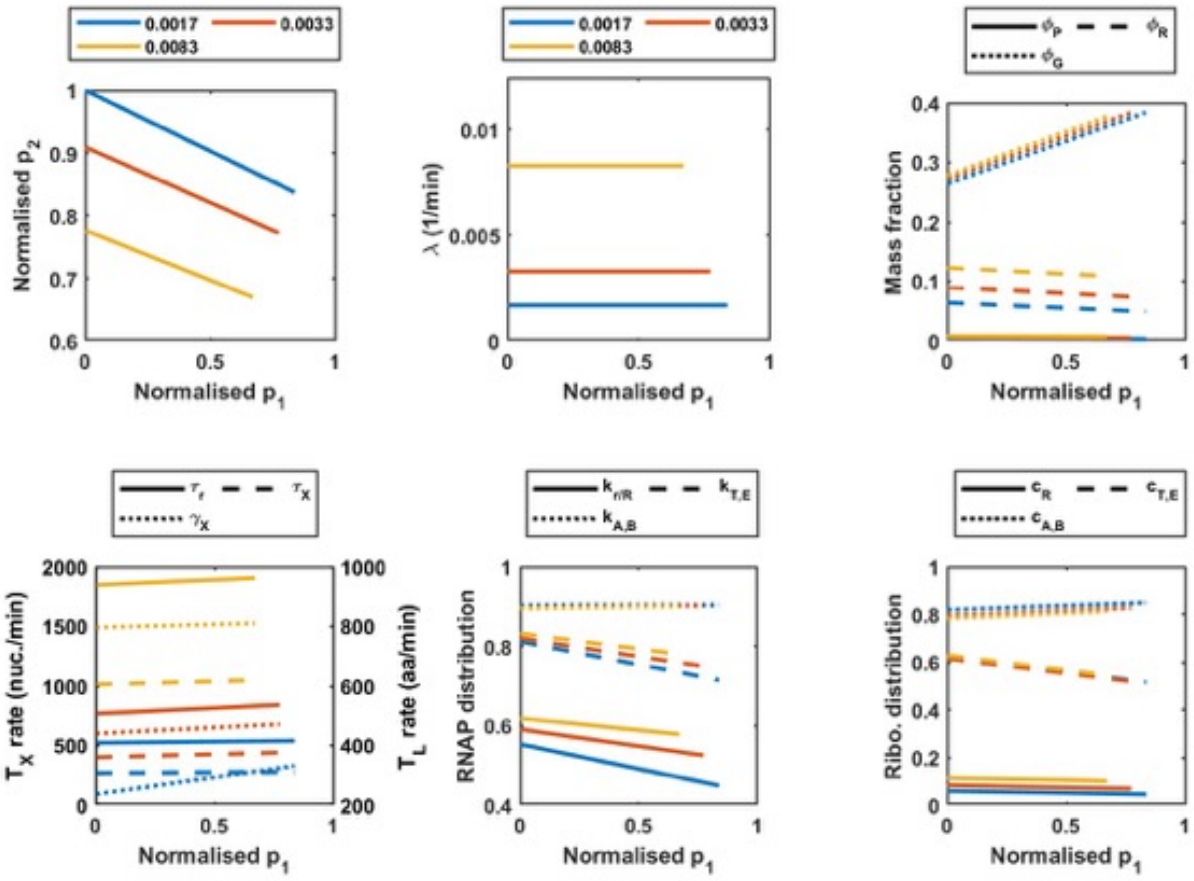

Figure S2. Full simulation results from Figure 2. Simulations of the steady state concentration of RFP and GFP, normalised by maximum protein production for a different growth rates. Simulations were carried out as described in the main text. **(A)** Protein output. **(B)** Growth rate. **(C)** The mass fraction of the RNA polymerase (Φ_P), ribosomes (Φ_R) and circuit proteins (Φ_G). **(D)** The mRNA (τ_X) and rRNA (τ_r) transcription elongation rate (plotted on the left axis, T_X rate) and peptide elongation rate (γ_X) (plotted on the right axis, T_L rate). **(E)** Proportion of transcribing RNA polymerases transcribing rRNA and r-protein genes ($k_{r,R}$), enzymes ($k_{T,E}$) and circuit genes ($k_{A,B}$) **(F)** Proportion of translating ribosomes translating r-proteins (c_R), enzymes ($c_{T,E}$) and circuit genes ($c_{A,B}$).

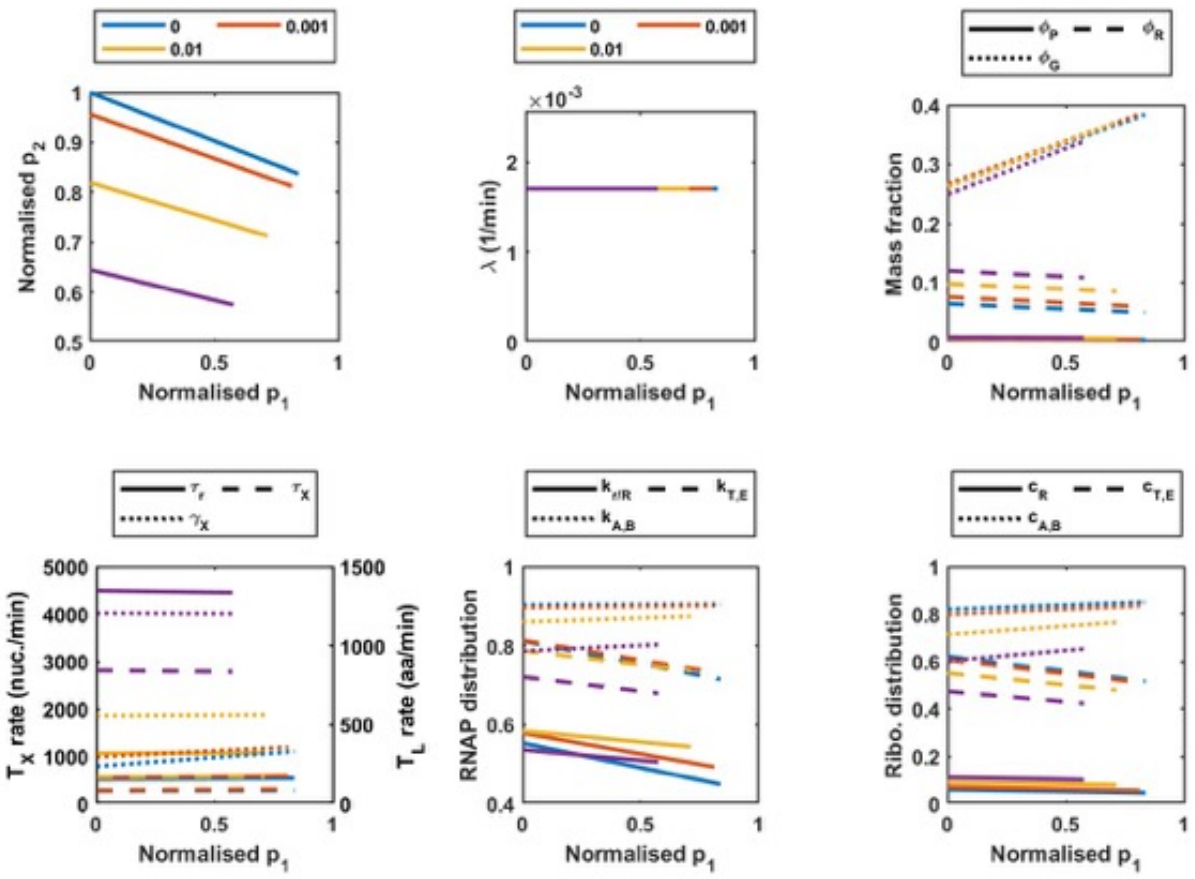

Figure S3. Full simulation results from Figure 3. Simulations of the steady state concentration of RFP and GFP, normalised by maximum protein production for a different RNA polymerase inhibition rates, k_{rf}. Simulations were carried out as described in the main text. **(A)** Protein output. **(B)** Growth rate. **(C)** The mass fraction of the RNA polymerase (Φ_P), ribosomes (Φ_R) and circuit proteins (Φ_G). **(D)** The mRNA (τ_X) and rRNA (τ_r) transcription elongation rate (plotted on the left axis, T_X rate) and peptide elongation rate (γ_X) (plotted on the right axis, T_L rate). **(E)** Proportion of transcribing RNA polymerases transcribing rRNA and r-protein genes ($k_{r,R}$), enzymes ($k_{T,E}$) and circuit genes ($k_{A,B}$) **(F)** Proportion of translating ribosomes translating r-proteins (c_R), enzymes ($c_{T,E}$) and circuit genes ($c_{A,B}$).

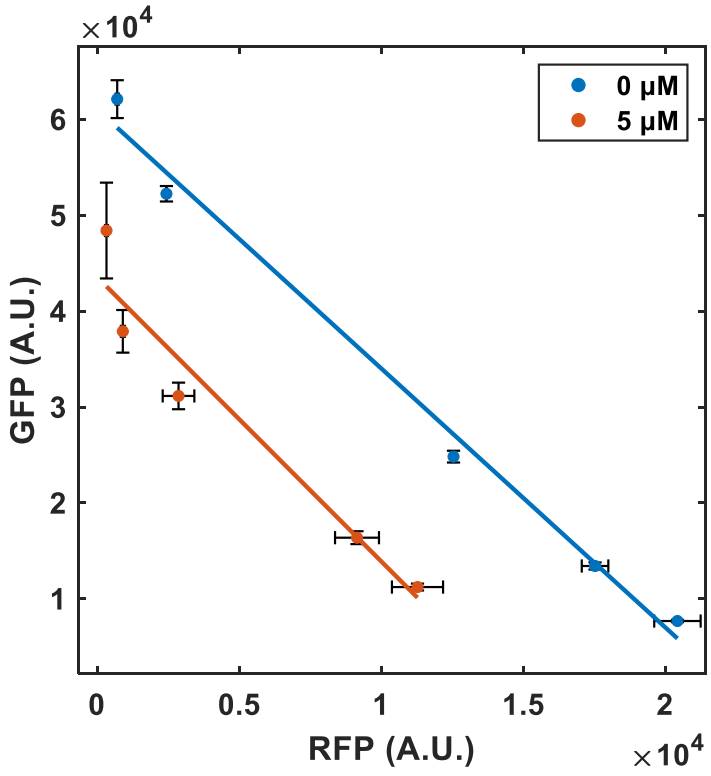

Figure S4. Effect of selective inhibition of translation on the two-reporter circuit gene expression. To characterize heterologous gene expression profile and the gene expression coupling under partial inhibition of translation, the dual reporter strain was grown in the chemostat at a set growth rate in the presence of a sublethal concentration of chloramphenicol (shown in the box) and different concentrations of AHL.

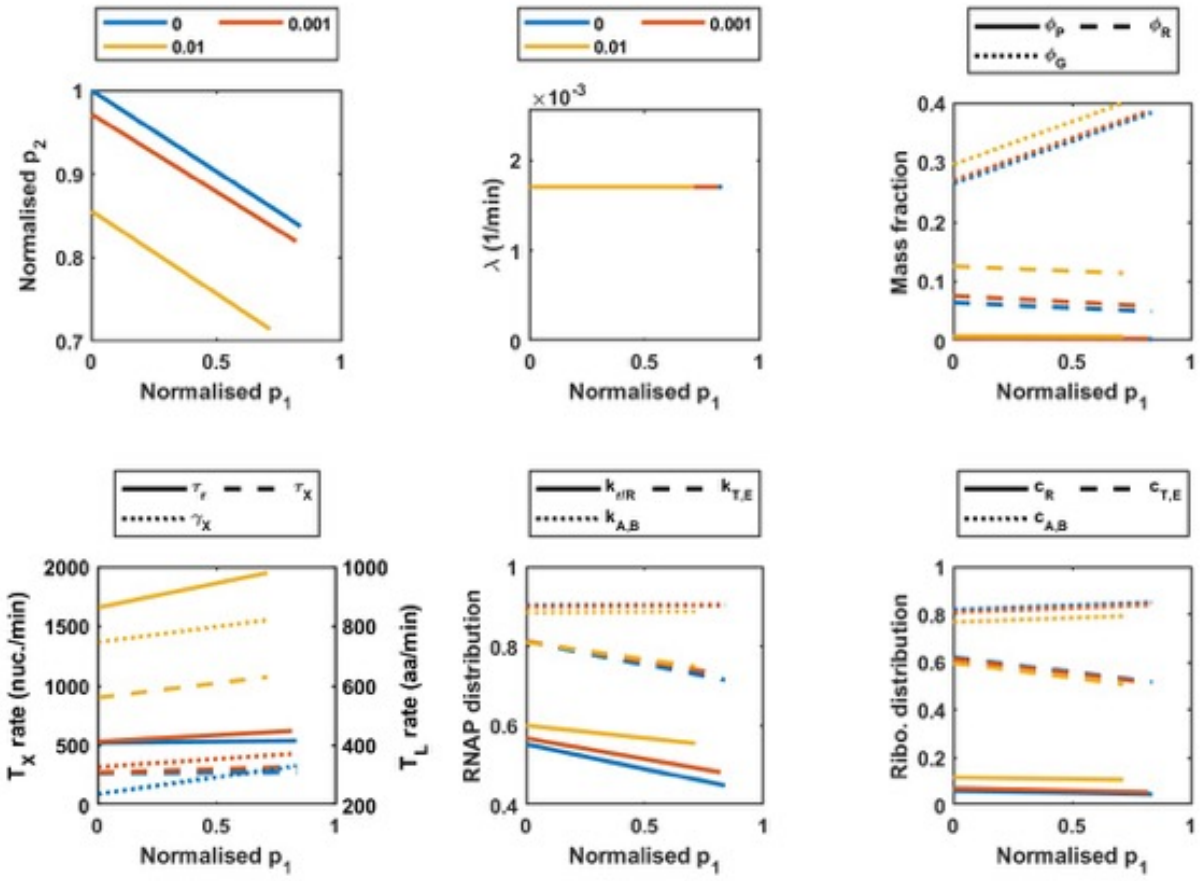

Figure S5 Full simulation results for ribosome inhibition. Simulations of the steady state concentration of RFP and GFP, normalised by maximum protein production for a different ribosome inhibition rates, k_{cm}. Simulations were carried out as described in the main text. **(A)** Protein output. **(B)** Growth rate. **(C)** The mass fraction of the RNA polymerase (Φ_P), ribosomes (Φ_R) and circuit proteins (Φ_G). **(D)** The mRNA (τ_X) and rRNA (τ_r) transcription elongation rate (plotted on the left axis, T_X rate) and peptide elongation rate (γ_X) (plotted on the right axis, T_L rate). **(E)** Proportion of transcribing RNA polymerases transcribing rRNA and r-protein genes ($k_{r,R}$), enzymes ($k_{T,E}$) and circuit genes ($k_{A,B}$) **(F)** Proportion of translating ribosomes translating r-proteins (c_R), enzymes ($c_{T,E}$) and circuit genes ($c_{A,B}$).

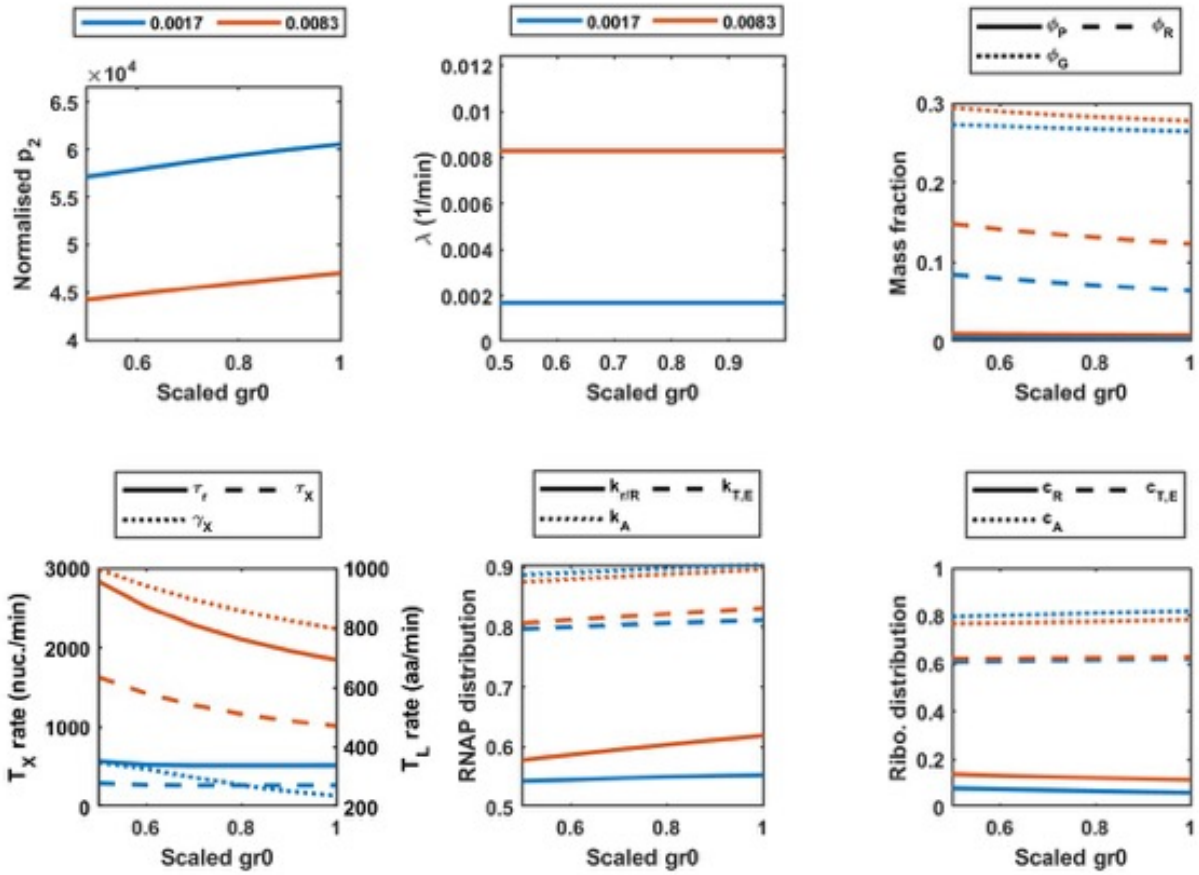

Figure S6. Full simulation results from Figure 4. Simulations of the steady state concentration of RFP and GFP for a different rRNA expression rates. Simulations were carried out as described in the main text. **(A)** Protein output. **(B)** Growth rate. **(C)** The mass fraction of the RNA polymerase (Φ_P), ribosomes (Φ_R) and circuit proteins (Φ_G). **(D)** The mRNA (τ_X) and rRNA (τ_r) transcription elongation rate (plotted on the left axis, T_X rate) and peptide elongation rate (γ_X) (plotted on the right axis, T_L rate). **(E)** Proportion of transcribing RNA polymerases transcribing rRNA and r-protein genes ($k_{r,R}$), enzymes ($k_{T,E}$) and circuit genes ($k_{A,B}$) **(F)** Proportion of translating ribosomes translating r-proteins (c_R), enzymes ($c_{T,E}$) and circuit genes ($c_{A,B}$).

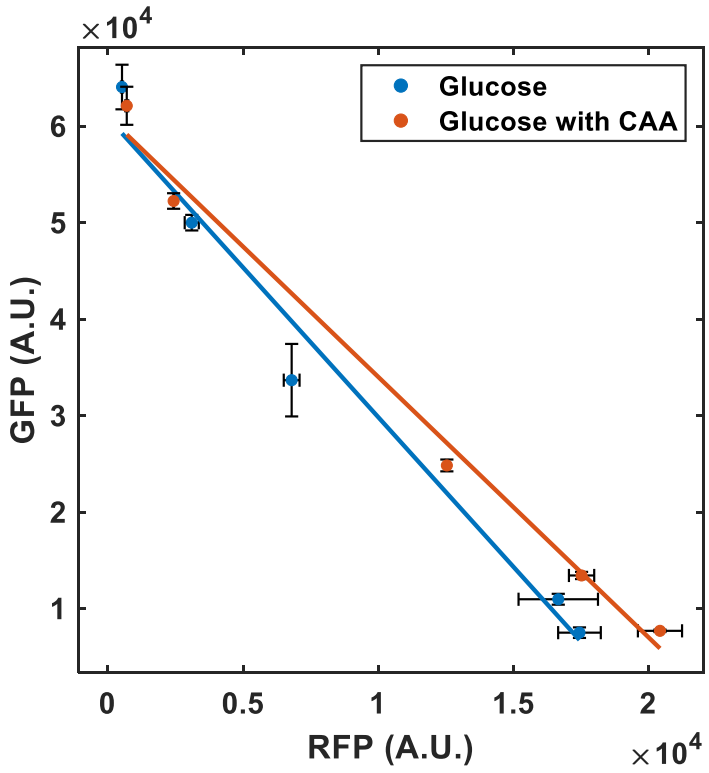

Figure S7. Effect of additional nutrients on the circuit gene expressions. The dual reporter strain was cultured in the continuous system containing M9 minimal medium supplemented with glucose as a sole carbon source. To determine the level of the gene expression coupling, different concentration of AHL applied into each bioreactor and measured both GFP and RFP intensities. The counterpart expression profile from Figure 2A also displayed in this figure.

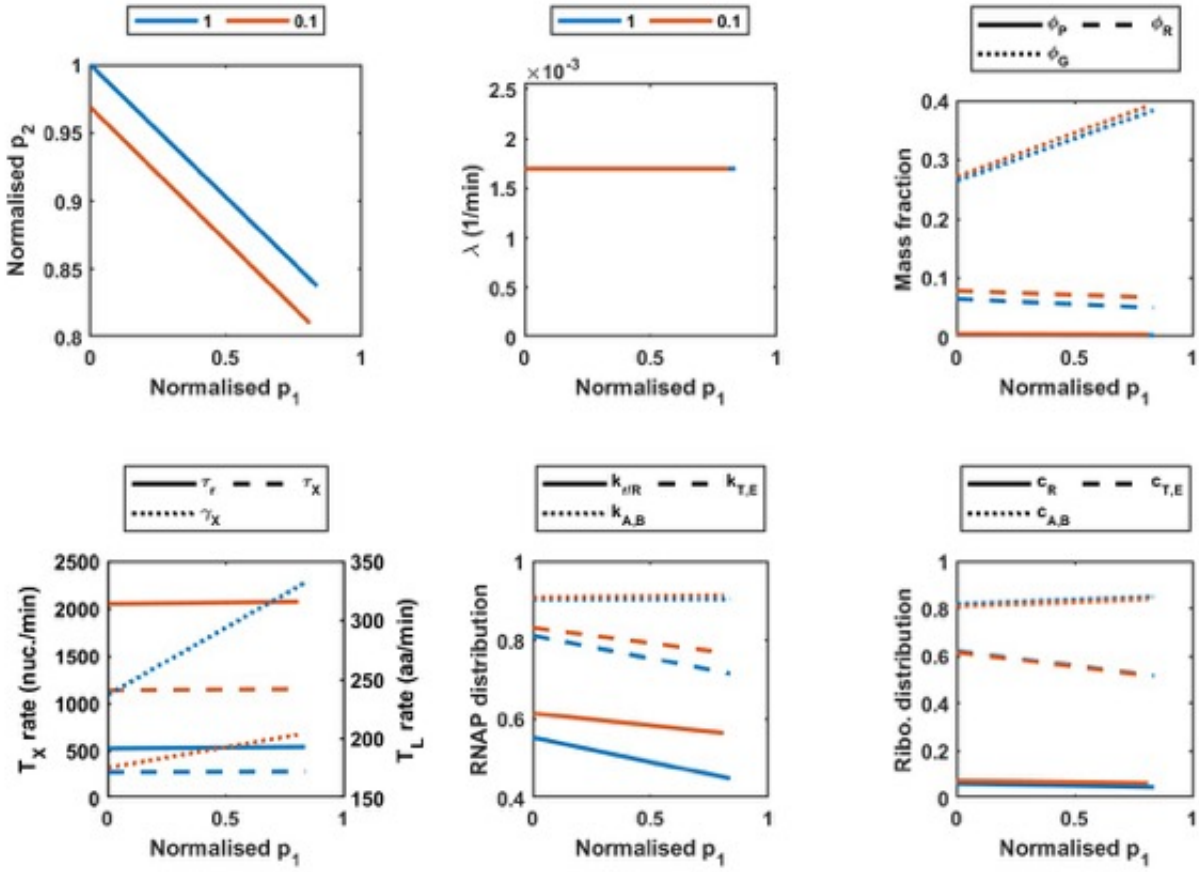

Figure S8. Full simulation results from Figure 5. Simulations of the steady state concentration of RFP and GFP for a different ϕ_a values. Simulations were carried out as described in the main text. **(A)** Protein output. **(B)** Growth rate. **(C)** The mass fraction of the RNA polymerase (Φ_P), ribosomes (Φ_R) and circuit proteins (Φ_G). **(D)** The mRNA (τ_X) and rRNA (τ_r) transcription elongation rate (plotted on the left axis, T_X rate) and peptide elongation rate (γ_X) (plotted on the right axis, T_L rate). **(E)** Proportion of transcribing RNA polymerases transcribing rRNA and r-protein genes ($k_{r,R}$), enzymes ($k_{T,E}$) and circuit genes ($k_{A,B}$) **(F)** Proportion of translating ribosomes translating r-proteins (c_R), enzymes ($c_{T,E}$) and circuit genes ($c_{A,B}$).

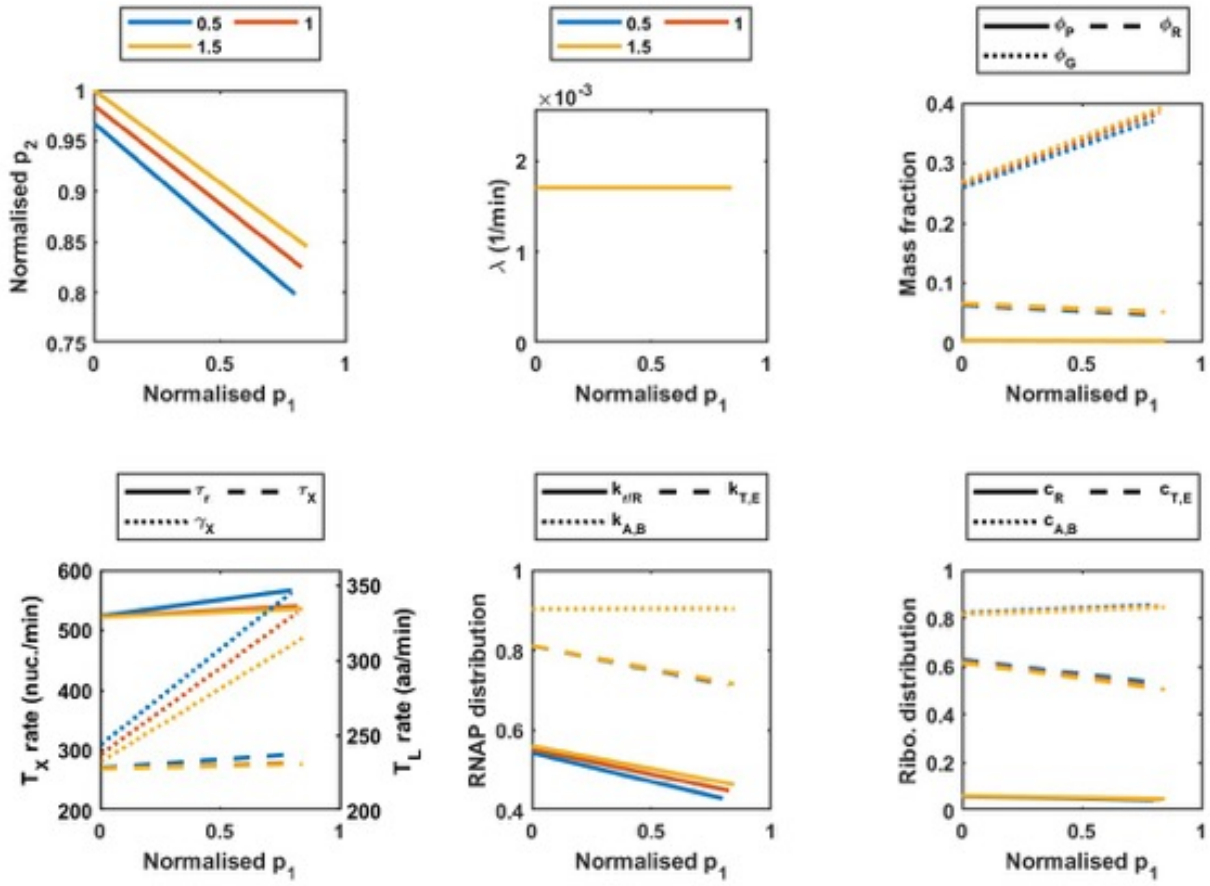

Figure S9. Full simulation results for varying o_X. Simulations of the steady state concentration of RFP and GFP for a 0.5, 1 and 1.5 times the nominal value of o_X. Simulations were carried out as described in the main text. **(A)** Protein output. **(B)** Growth rate. **(C)** The mass fraction of the RNA polymerase (Φ_P), ribosomes (Φ_R) and circuit proteins (Φ_G). **(D)** The mRNA (τ_X) and rRNA (τ_r) transcription elongation rate (plotted on the left axis, T_X rate) and peptide elongation rate (γ_X) (plotted on the right axis, T_L rate). **(E)** Proportion of transcribing RNA polymerases transcribing rRNA and r-protein genes ($k_{r,R}$), enzymes ($k_{T,E}$) and circuit genes ($k_{A,B}$) **(F)** Proportion of translating ribosomes translating r-proteins (c_R), enzymes ($c_{T,E}$) and circuit genes ($c_{A,B}$).

Table S1. Bacterial strains, plasmids and oligonucleotides used in this study

***E. coli* strains**	**Description**	**Reference**
MG1655	F^-, λ^-, *ilvG*$^-$, *rfb-50*, *rph-1*	(Blattner *et al*, 1997)
MG1655 L9-*msf*GFP	MG1655 derivative with a C-terminal msf GFP tag in 50S ribosomal protein L9, encoded by *rplI* gene	This study
BW25113	Parental strain for the Keio Collection of single gene knockouts Δ(*araD-araB*)567,Δ*lacZ4787*(::*rrnB-3*), λ-, *rph-1*, Δ(*rhaD-rhaB*)568, *hsdR514*	(Baba *et al*, 2006)
BW25113 (Δ relA)	BW25113 derivate with a deletion of *relA* genes	Keio collection
BW25113 (Δ spoT)	BW25113 derivate with a deletion of *spoT* genes	This study
DH5α	Cloning host: F^- Φ80 *lacZ*Δ*M*Δ15 (*lacZYA-argF*), U169, *recA1, endA1, hsdR17, R-M+, supE44, thil, gyrA, relA1*	(Hanahan & Meselson, 1983)
DH5α λpir	DH5α λpir phage lysogen	Victor de Lorenzo's collection
SQ37	MG1655 derivate, Δ*rrnE*	(Quan *et al*, 2015)
SQ40	MG1655 derivate, Δ*rrnEG*	(Quan *et al.*, 2015)
SQ49	MG1655 derivate, Δ*rrnGBA*	(Quan *et al.*, 2015)
SQ53	MG1655 derivate, Δ*rrnGBAD*	(Quan *et al.*, 2015)
SQ78	MG1655 derivate, Δ*rrnGADE*	(Quan *et al.*, 2015)
Plasmid	**Description**	**Reference**
pEMG	Suicide plasmid, Km^R, oriR6K, *lacZa* with two flanking I-SceI sites	(Martinez-Garcia & de Lorenzo, 2011)
pEMG-rplI-msfGFP	Same as pEMG but carrying the msf GFP gene with upstream and downstream flanking regions of the C-terminus of *E. coli* rplI gene	This study
pKD4	Template for Km cassette, oriR6Kgamma, *bla, aphA*	(Datsenko & Wanner, 2000)
pKD46	Red recombinase expression vector, repA101ts, oriR101, P_{araB} *exo, bet, gam araC bla*	(Datsenko & Wanner, 2000)
pSEVA63-Dual	pSEVA631 carrying the circuit MBP 1.0	(Darlington *et al*, 2018)

Oligos	Sequence (5' --> 3')
TS1^{rplI}F	AGGGATAACAGGGTAATCTGCGCTCGCTACCTGTCCCTGCT
TS1^{rplI}R	TTTACTGCCACCGCCACCGCTTTCAGCTACTACGTTTACGA
rplI-msfGFP-F	GAAAGCGGTGGCGGTGGCAGTAAAGGTGAAGAACTGTTCACCG
rplI-msfGFP-R	TACGTCTCGTTGAATAACGAATTATTTGTAGAGTTCATCCAT
TS2^{rplI}F	CATGGATGAACTCTACAAATAATTCGTTATTCAACGAGACGT
TS2^{rplI}R	GCCTGCAGGTCGACTCTAGAGTATTTATTGCAAGATGTCGAAT
spoT KO F	TTACCGCTATTGCTGAAGGTCGTCGTTAATCACAAAGCGGGTCGC CCTTGGTGTAGGCTGGAGCTGCTTC
spoT KO R	CGTGCATAACGTGTTGGGTTCATAAAACATTAATTTCGGTTTCGG GTGACATGGGAATTAGCCATGGTCC

Supplementary references

Baba T, Ara T, Hasegawa M, Takai Y, Okumura Y, Baba M, Datsenko KA, Tomita M, Wanner BL, Mori H (2006) Construction of *Escherichia coli* K-12 in-frame, single-gene knockout mutants: the Keio collection. *Mol. Syst. Biol.* 2: 2006 0008

Blattner FR, Plunkett G, 3rd, Bloch CA, Perna NT, Burland V, Riley M, Collado-Vides J, Glasner JD, Rode CK, Mayhew GF *et al* (1997) The complete genome sequence of *Escherichia coli* K-12. *Science* 277: 1453-1462

Bremer H, Dennis PP (1996) Modulation of chemical composition and other parameters of the cell by growth rate. ASM Press, Washington, D.C

Darlington APS, Kim J, Jimenez JI, Bates DG (2018) Dynamic allocation of orthogonal ribosomes facilitates uncoupling of co-expressed genes. *Nat. Commun.* 9:695

Datsenko KA, Wanner BL (2000) One-step inactivation of chromosomal genes in *Escherichia coli* K-12 using PCR products. *Proc. Natl. Acad. Sci. U.S.A.* 97: 6640-6645

Hanahan D, Meselson M (1983) Plasmid screening at high colony density. *Methods Enzymol.* 100: 333-342

Martinez-Garcia E, de Lorenzo V (2011) Engineering multiple genomic deletions in Gram-negative bacteria: analysis of the multi-resistant antibiotic profile of *Pseudomonas putida* KT2440. *Environ. Microbiol.* 13: 2702-2716

Quan S, Skovgaard O, McLaughlin RE, Buurman ET, Squires CL (2015) Markerless *Escherichia coli rrn* deletion strains for genetic determination of ribosomal binding sites. *G3 (Bethesda)* 5: 2555-2557